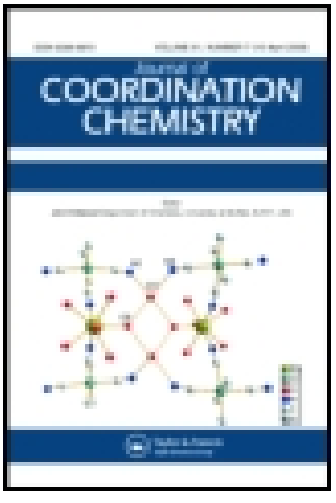

Journal of Coordination Chemistry
Publication details, including instructions for authors and subscription information:
http://www.tandfonline.com/loi/gcoo20

Synthesis, structural characterization, oxygen sensitivity, and antimicrobial activity of ruthenium(II) carbonyl complexes with thiosemicarbazones

Nurdan Öztürk[a], Pelin Köse Yaman[b], Murat Yavuz[cd], Özlem Öter[b], Suna Timur[c] & Elif Subaşi[b]

[a] The Graduate School of Natural and Applied Sciences, Dokuz Eylül University, İzmir, Turkey

[b] Faculty of Science, Department of Chemistry, Dokuz Eylül University, İzmir, Turkey

[c] Faculty of Science, Department of Biochemistry, Ege University, İzmir, Turkey

[d] Faculty of Science, Department of Chemistry, Dicle University, Diyarbakir, Turkey

Accepted author version posted online: 28 Jul 2014.Published online: 20 Aug 2014.

To cite this article: Nurdan Öztürk, Pelin Köse Yaman, Murat Yavuz, Özlem Öter, Suna Timur & Elif Subaşi (2014): Synthesis, structural characterization, oxygen sensitivity, and antimicrobial activity of ruthenium(II) carbonyl complexes with thiosemicarbazones, Journal of Coordination Chemistry, DOI: 10.1080/00958972.2014.948433

To link to this article: http://dx.doi.org/10.1080/00958972.2014.948433

Journal of Coordination Chemistry, 2014
http://dx.doi.org/10.1080/00958972.2014.948433

Synthesis, structural characterization, oxygen sensitivity, and antimicrobial activity of ruthenium(II) carbonyl complexes with thiosemicarbazones

NURDAN ÖZTÜRK†, PELIN KÖSE YAMAN‡, MURAT YAVUZ§¶, ÖZLEM ÖTER‡, SUNA TIMUR§ and ELIF SUBAŞI*‡

†The Graduate School of Natural and Applied Sciences, Dokuz Eylül University, İzmir, Turkey
‡Faculty of Science, Department of Chemistry, Dokuz Eylül University, İzmir, Turkey
§Faculty of Science, Department of Biochemistry, Ege University, İzmir, Turkey
¶Faculty of Science, Department of Chemistry, Dicle University, Diyarbakir, Turkey

(*Received 25 March 2014; accepted 26 June 2014*)

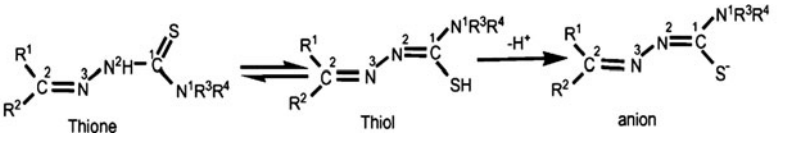

Ru(II) carbonyl complexes were prepared by reacting $[Ru(H)(Cl)(CO)(PPh_3)_3]$ with the respective thiosemicarbazone ligands and the complexes were characterized by UV–vis, FT-IR, and ^1H and ^{31}P NMR spectroscopy. Oxygen sensitivities and antimicrobial activities of the complexes were determined.

$[Ru(CO)(PPh_3)_2(\eta^3\text{-}O,N^3,S\text{-}TSC^1)]$ (**1**), $[Ru(Cl)(CO)(PPh_3)_2(\eta^2\text{-}N^3,S\text{-}TSC^2)]$ (**2**), and $[Ru(Cl)(CO)(PPh_3)_2(\eta^2\text{-}N^3,S\text{-}TSC^3)]$ (**3**) have been prepared by reacting $[Ru(H)(Cl)(CO)(PPh_3)_3]$ with the respective thiosemicarbazones TSC^1 (*2-hydroxy-3-methoxybenzaldehyde thiosemicarbazone*), TSC^2 (*3-hydroxybenzaldehyde thiosemicarbazone*), and TSC^3 (*3,4-dihydroxybenzaldehyde thiosemicarbazone*) in a 1 : 1 M ratio in toluene and all of the complexes have been characterized by UV–vis, FT-IR, and ^1H and ^{31}P NMR spectroscopy. The spectroscopic studies showed that TSC^1 is coordinated to the central metal as a tridendate ligand coordinating via the azomethine nitrogen (C=N), phenolic oxygen, and sulfur to ruthenium in **1**, whereas TSC^2 and TSC^3 are coordinated to ruthenium as a bidentate ligand through azomethine nitrogen (C=N) and sulfur in **2** and **3**. Oxygen sensitivities of **1–3** and $[Ru(Cl)(CO)(PPh_3)_2(\eta^2\text{-}N^3,S\text{-}TSC^4)]$ (**4**), and antimicrobial activities of **1–3** have been determined.

Keywords: Ruthenium(II) carbonyl complexes; Thiosemicarbazones; Oxygen sensitivity; Antimicrobial activities

1. Introduction

Complexes of transition metals containing ligands with N, S or N, S, O donors exhibit interesting stereochemical, electrochemical, and electronic properties [1, 2]. Derivatives of semicarbazones and thiosemicarbazones (TSCs) are widely studied nitrogen and oxygen/sulfur

*Corresponding author. Email: elif.subasi@deu.edu.tr

donors [3, 4]. Particularly, TSCs are an important class of sulfur donor ligands because of their mixed hard–soft donor character and versatile coordination behavior [5]. TSCs exist as thione–thiol tautomers and can bind to a metal in neutral or anionic forms. The anionic form is produced after loss of $-N^2H$ or –SH hydrogen ions. A number of bonding modes have been observed for TSCs in their neutral or anionic forms as shown in figure 1.

TSCs usually react as chelating ligands with transition metal ions by bonding through sulfur and azomethine nitrogen and in some cases they behave as tridentate ligands and bond through sulfur and two nitrogens [6]. TSCs and their metal complexes have become the subjects of severe study because of their wide-ranging biological activities (antitumor, antibacterial, antiviral, antiamoebic, and antimalarial activities), analytical applications, and interesting chemical and structural properties [7–9].

Medicinal chemistry has focused on TSCs due to their biological activities demonstrated by various derivatives incorporating the heterocyclic moiety [10–12]. Owing to their chemistry, versatile activity, and prospective use as drugs, they have ample interest [13, 14]. For transition metal complexes, decreased or increased biological activities are reported [15–17]. Complexes of ruthenium with TSCs, which can coordinate either in neutral thione form or in the anionic thiolate form, have received attention for varied coordination modes [18].

Use of ruthenium complexes as chemotherapeutic agents for treatment of cancer is well established [19]. Recently, an oligomer of thiophene-2-carboxaldehyde thiosemicarbazone was electrochemically deposited on graphite surfaces as the matrix for enzyme immobilization [20]. The biosensing applicability and evaluation as antimicrobial agents of [(η^6-*p*-cymene)RuClTSC^{N-S}]Cl and [Ru(CO)Cl(PPh_3)$_2$TSC^{N-S}] (**4**) were investigated using glucose oxidase as a model enzyme [21]. Ruthenium complexes are widely used for oxygen-sensing purposes due to the fact that they produce metal-to-ligand charge-transfer excited states which are readily quenched by oxygen. They are preferred for their high quantum yields, fast response times, strong visible absorptions, large Stoke's shifts, and high photophysical and photochemical stabilities [22–24]. In this study, we have also investigated the applicability of the complexes for oxygen-sensing purposes.

As ligands, TSCs have more than one potential donor. Therefore, we tried to observe the sites of substitution of these ligands to the metal center. Our continued interest in the synthesis and structural aspects of ruthenium(II) led us to launch an exploratory investigation into the behavior of [Ru(H)(Cl)(CO)(PPh_3)$_3$] with TSC$^{1–3}$. As an extension of our previous studies, herein, we describe the synthesis and full characterization of [Ru(CO)(PPh_3)$_2$(η^3-*O,N*^{3},*S*-TSC^1)] (**1**), [Ru(Cl)(CO)(PPh_3)$_2$(η^2-*N*^{3},*S*-TSC^2)] (**2**), and [Ru(Cl)(CO)(PPh_3)$_2$(η^2-*N*^{3},*S*-TSC^3)] (**3**) which have been prepared by reacting [Ru(H)(Cl)(CO)(PPh_3)$_3$] with the respective thiosemicarbazone ligands TSC^1 (*2-hydroxy-3-methoxybenzaldehyde thiosemicarbazone*), TSC^2 (*3-hydroxybenzaldehyde thiosemicarbazone*), and TSC^3 (*3,4-dihydroxybenzaldehyde thiosemicarbazone*). The complexes were elucidated by

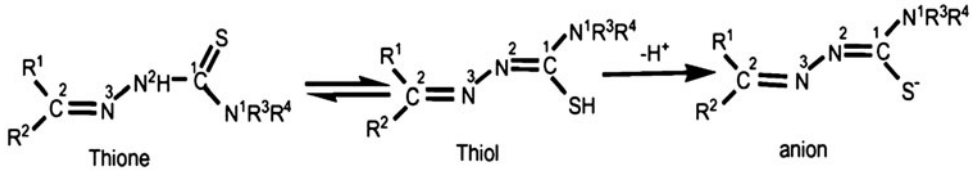

Figure 1. Thione and thiol forms of TSCs.

elemental analysis, FT-IR, UV–vis spectroscopy, and a combination of multinuclear NMR spectroscopy. Oxygen sensitivities and antimicrobial effects of these complexes are also investigated.

2. Experimental

2.1. *Chemicals and physical measurements*

Toluene, ethanol, petroleum ether, dichloromethane, and silica gel were purchased from Merck and $RuCl_3 \cdot 3H_2O$ was purchased from Aldrich. These reagents were used as supplied. The solvents used were purified and distilled according to routine procedures [25]. Ethyl cellulose was from Organics with an ethoxy content of 48%. The plasticizer dioctyl phthalate (DOP) was from Aldrich. The ionic liquid (IL) 1-ethyl-3-methylimidazolium tetrafluoroborate ($[EMIM^+][BF_4^-]$) was from Fluka. Oxygen and nitrogen gas cylinders were of 99.9% purity and obtained from Linde Company, Izmir, Turkey.

Reactions were carried out under dry nitrogen using Schlenk techniques. All solvents were dried and degassed prior to use. Elemental analyses were carried out using a LECO-CHNS-O-9320 by Technical and Scientific Research Council of Turkey, TUBITAK. IR spectra on a Varian 1000 FT spectrophotometer and UV–vis Spectra Shimadzu Model 1800 spectrophotometer were recorded on samples at the Dokuz Eylül University. ^1H and ^{31}P NMR spectra were recorded in DMSO-d_6 on 500 MHz High Performance Digital FT NMR at Ege University.

2.2. *Synthesis of the compounds*

2.2.1. Synthesis of the ligands. The preparative methods for TSCs were well described by Klayman *et al.* [26] and Scovill [27]. In general, a thiosemicarbazide was dissolved in methanol by refluxing for half an hour; however, sometimes, a few milliliters of distilled water are added to completely dissolve it. After addition of a given aldehyde or ketone, the reaction mixture is refluxed for 8–10 h and evaporation gave crude sample which was recrystallized from methanol.

2.2.2. Synthesis of the complexes. Complexes **1–4** were prepared by reacting $[Ru(H)(Cl)(CO)(PPh_3)_3]$ with the respective thiosemicarbazone ligands TSC^{1-4} and were obtained in 75–80% yields. The methods employed for the preparation of **1–3** are very similar, so that the preparation of $[Ru(CO)(PPh_3)_2(\eta^3\text{-}O,N^3,S\text{-}TSC^1)]$, **1** is given in detail as a representative example. $[Ru(Cl)(CO)(PPh_3)_2(\eta^2\text{-}N^3,S\text{-}TSC^4)]$, **4**, was prepared according to the published results [21].

2.2.2.1. *$[Ru(CO)(PPh_3)_2(\eta^3\text{-}O,N^3,S\text{-}TSC^1)]$ (1).* To a solution of $[Ru(H)(Cl)(CO)(PPh_3)_3]$ (950 mg, 1 mM) in toluene (25 mL) TSC^1 (225 mg) was added. The mixture was refluxed for 5 h under nitrogen. The resulting solution was concentrated to 5 mL and the product was separated by addition of a small amount of petroleum ether. It was filtered and dried *in vacuo*. The composition of the compounds is confirmed by elemental analysis. Yield (80%). Found: C, 62.75; H, 4.75; N, 4.71; S, 3.59. Calcd for $C_{46}H_{42}N_3O_3P_2RuS$: C, 62.79; H, 4.81; N, 4.78; S, 3.64. FT-IR (ν, KBr): 3148 (s, N–H), 1586 (m, C=N), 719 (w, C–S), 1093

(w, CN, NCN), 1944 (s, C≡O) cm^{-1}. ^1H NMR (500 MHz, δ, DMSO-d_6): 8.54 (1H, s, N–H), 8.38 (1H, s, HC=N), 6.74–8.08 (3H, m, Ar–H) ppm. ^{31}P NMR: 27.61. UV–vis (THF) (nm) (A): λ_1: 281.0 (0.212).

2.2.2.2. *[Ru(Cl)(CO)(PPh_3)$_2$(η^2-N^3,S-TSC^2)] (2).* A similar synthetic procedure as that used for **1** was used except that TSC^1 was replaced by TSC^2 (195 mg), giving orange crystals. The composition of the compound is confirmed by elemental analysis. Yield (75%). Found: C, 61.02; H, 4.26; N, 4.70; S, 3.60. Calcd for $C_{45}H_{39}ClN_3O_2P_2RuS$: C, 61.12; H, 4.45; N, 4.75; S, 3.63. FT-IR (ν, KBr): 1587 (m, C=N), 744 (m, C–S), 1092 (w, CN, NCN), 1955 (s, C≡O) cm^{-1}. ^1H NMR (500 MHz, δ, DMSO-d_6): 8.37 (1H, s, HC=N), 6.79–7.96 (3H, m, Ar–H) ppm. ^{31}P NMR: 55.01, 43.52. UV–vis (THF) (nm) (A): λ_1: 284.0 (0.138).

2.2.2.3. *[Ru(Cl)(CO)(PPh_3)$_2$(η^2-N^3,S-TSC^3)] (3).* A similar synthetic procedure as that used for **1** was used except that TSC^1 was replaced by TSC^3 (211 mg), giving orange crystals. The composition is confirmed by elemental analysis. Yield (79%). Found: C, 60.01; H, 4.35; N, 4.60; S, 3.51. Calcd for $C_{45}H_{39}ClN_3O_3P_2RuS$: C, 60.03; H, 4.37; N, 4.67; S, 3.56. FT-IR (ν, KBr): 1592 (m, C=N), 742 (w, C–S), 1113 (w, CN, NCN), 1935 (s, C≡O) cm^{-1}. ^1H NMR (500 MHz, δ, DMSO-d_6): 8.30 (1H, s, HC=N), 6.74–7.17(3H, m, Ar–H) ppm. ^{31}P NMR: 36.73 ppm. UV–vis (THF) (nm) (A): λ_1: 267.0 (0.299).

2.3. *Preparation of thin films*

The sensing cocktail was prepared by mixing 240 mg of ethyl cellulose (ethoxy content of 48%) polymer, 192 mg of plasticizer (DOP), 10 mg of dye, 48 mg of ionic liquid, 1-ethyl-3-methylimidazolium tetrafluoroborate, in tetrahydrofuran (THF). After homogenation of the cocktail under magnetic stirring, the cocktail was spread onto a 125 μm polyester support (Mylar TM type) by knife coating technique and located in a THF-saturated desiccator. Thicknesses of the films were measured using a Tencor Alpha Step 500 Prophylometer and were found to be 5.43 μm. This result was an average of eight measurements and exhibited a standard deviation of ±0.12. Each sensing film was cut to 1.2 cm diameter, fixed in the cell, and the emission and excitation spectra were recorded.

2.4. *Fluorescence-based studies*

Steady-state fluorescence emission and excitation spectra were measured using a Varian Cary Eclipse Spectrofluorometer with a Xenon flash lamp as the light source. The excitation and emission slits were set to 20 nm and the detector voltage was set to 600 V.

2.5. *Gas-sensing studies*

The gases O_2 and N_2 were mixed in the concentration range of 0.0–100.0% in a Sonimix 7000A gas blending system. The output flow rate of the gas mixture was maintained at 550 mL min^{-1}. The gases were introduced on the sensing slides in a covered cuvette via a diffuser needle under ambient conditions. Excitation and emission spectra of the sensing materials were recorded after exposure to certain concentrations of oxygen.

2.6. *Test for antimicrobial activity*

The antimicrobial activity of $[Ru(CO)(PPh_3)_2(\eta^3\text{-}O,N^3,S\text{-}TSC^1)]$ (**1**), $[Ru(Cl)(CO)(PPh_3)_2(\eta^2\text{-}N^3,S\text{-}TSC^2)]$ (**2**), and $[Ru(Cl)(CO)(PPh_3)_2(\eta^2\text{-}N^3,S\text{-}TSC^3)]$ (**3**) was evaluated using the disk diffusion test method according to the National Committee for Clinical Laboratory Standards [28] against the laboratory control strains belonging to the American Type Culture Collection (*Escherichia coli* ATCC 25,922, *Enterobacter cloacae* ATCC 23355, *Pseudomonas aeruginosa* ATCC 27853, *Bacillus subtilis* ATCC 11774, *Staphylococcus aureus* ATCC 25923, *Streptococcus pyogenes* ATCC 19615, and one fungus *Candida albicans* ATCC 10231) (LGC Standards GmbH, Wesel, Germany) and clinical isolate (*P. aeruginosa*, *S. aureus,* and *Streptococcus agalactiae* were kindly supplied from the Microbiology Department, Faculty of Medicine at the Dicle University).

The inocula of the test organisms were prepared by transferring three to five freshly grown colonies of the cultures into 25 mL of sterile Nutrient Broth (NB, Oxoid) and incubated at 37 °C for 4–5 h. The bacterial cultures were adjusted with 0.5 McFarand turbidity standards (1×10^8 CFU mL^{-1}) and streaked evenly onto the Nutrient Agar (NA, Oxoid) plate with a sterile cotton swab. Three to five colonies of *C. albicans* ATCC 10231 were inoculated into 25 mL of Sabouraud Dextrose Broth (SDB, Oxoid) and incubated at 37 °C for 8–10 h. *C. albicans* ATCC 10231 cultures were adjusted with 0.5 McFarand turbidity standards (1×10^8 CFU mL^{-1}) and streaked evenly onto the Sabouraud Dextrose Agar (SDA, Oxoid) plate with sterile cotton swabs [29]. Six–millimeter-diameter sterile filter paper disks (Oxoid, England) were impregnated with 10, 15, and 20 µL (at 5 mg mL^{-1}) of ruthenium complexes **1–3** solutions in dichloromethane/methanol (8 : 2) and were then dried 4 h on a clean Petri dish. The seeded plates were left for drying for 3–5 min, and the disks were placed on the agar using sterile forceps and were gently pressed down to ensure contact. Then the plates were incubated in an upright position at 37 °C for 24 h for bacteria and 48 h for fungi. Positive control (ofloxacin, 5 µg/disk (OFX); amoxycillin/clavulanic acid (2 : 1), 30 µg/disk (AMC); imipenem, 10 µg/disk (IMP); erythromycin, 15 µg/disk (E) (all from Oxoid) and nystatin, 60 µg/disk (N) (Sigma)) and negative control (disks imbued with 20 µL of DCM/MeOH (8 : 2) solvent system) were also included for each experiment. The diameters of zones of inhibition were determined in millimeters using an inhibition zone ruler and the results were recorded.

3. Results and discussion

3.1. *Synthesis*

Ruthenium(II) complexes $[Ru(CO)(PPh_3)_2(\eta^3\text{-}O,N^3,S\text{-}TSC^1)]$ (**1**), $[Ru(Cl)(CO)(PPh_3)_2(\eta^2\text{-}N^3,S\text{-}TSC^2)]$ (**2**), and $[Ru(Cl)(CO)(PPh_3)_2(\eta^2\text{-}N^3,S\text{-}TSC^3)]$ (**3**) have been prepared by reacting $[Ru(H)(Cl)(CO)(PPh_3)_3]$ with the respective thiosemicarbazone ligands TSC^1, TSC^2, and TSC^3 in a 1 : 1 M ratio in toluene and benzene (figure 2). The analytical data for **1–3** are summarized in the experimental section. The stoichiometry of the ligands and their complexes have been confirmed by elemental analyses. The spectroscopic data confirm that TSC^n (n = 1–3) coordinate thiosemicarbazone derivatives. For the structural characterization of TSC^n (n = 1–3) with their Ru(II) complexes **1–3**, FT-IR spectra, UV–vis spectra, and ^{1}H and ^{31}P NMR spectra were used and the corresponding data are given in the experimental section.

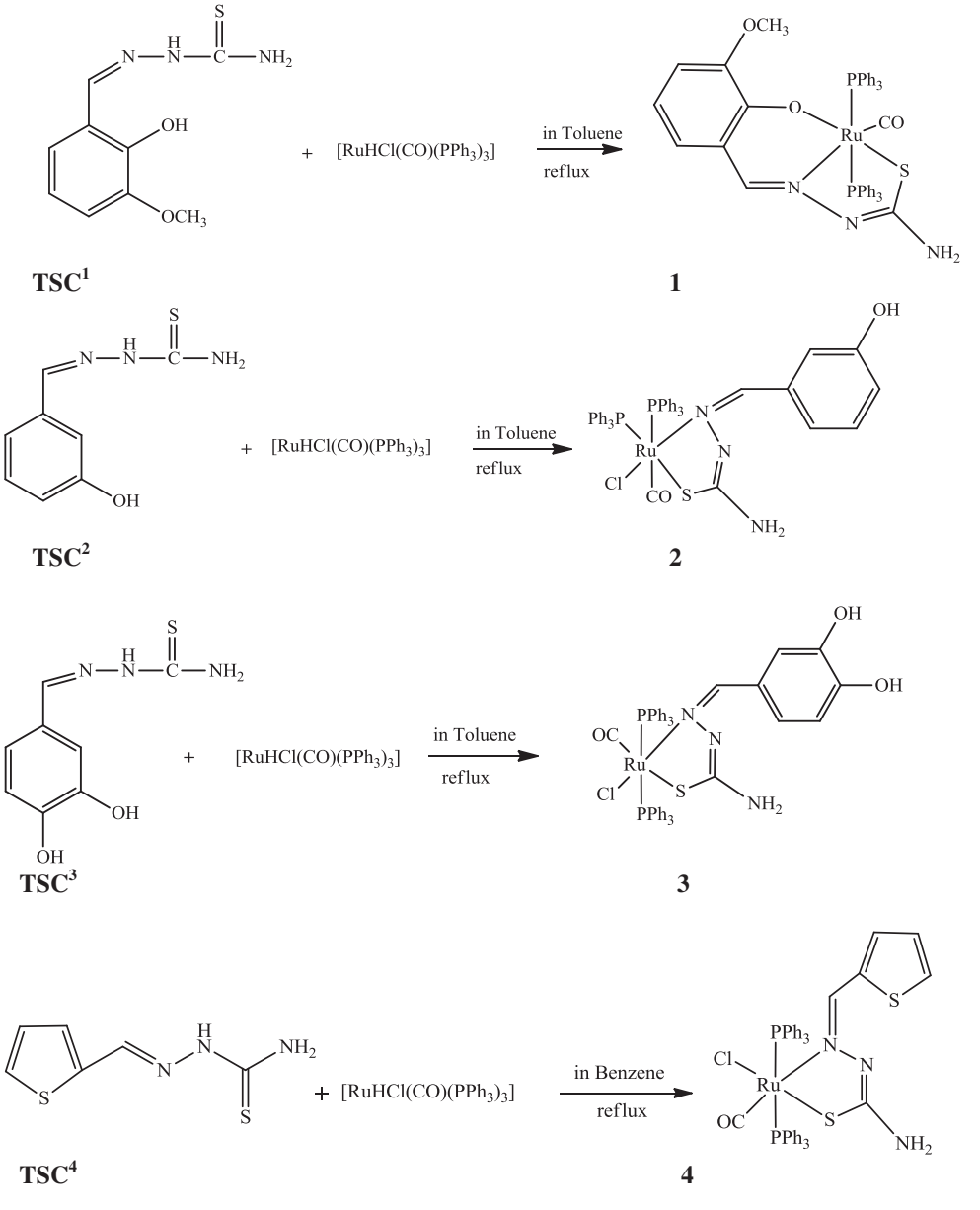

Figure 2. Structures of **1–4**.
Source: Taken from Ref. [21].

All the complexes were isolated in moderate yields and are quite stable in air and light. The analytical data for the complexes are in agreement with the formula proposed. The complexes are soluble in common organic solvents such as dimethyl sulphoxide, dichloromethane, and chloroform. Various attempts have been made to obtain single crystals of the complexes but were unsuccessful.

Based on elemental analysis and spectroscopic data, the complexes are best formulated as [Ru(CO)$(PPh_3)_2$(η^3-*O,N*^{3},*S*-TSC^1)] (**1**), [Ru(Cl)(CO)$(PPh_3)_2$(η^2-N^3,*S*-TSC^2)] (**2**), and [Ru(Cl)(CO)$(PPh_3)_2$(η^2-N^3,*S*-TSC^3)] (**3**). The spectroscopic data reasonably support the formulas of the compounds.

3.2. *Spectroscopic characterization*

3.2.1. Infrared spectra. TSCs can coordinate in a number of different manners. Most commonly they bind as either of two tautomeric forms, a neutral thione form or the anion from the thiol form. Infrared spectroscopy was used to confirm coordination as the thiol form in **1–3**. FT-IR spectra of the free ligands were compared with the complexes to confirm the coordination of the ligand to ruthenium. The main stretching frequencies of the FT-IR spectra of ligands TSC^{1-3} and Ru(II) complexes **1–3** are given in the experimental section.

The highest frequency bands at 3337 cm^{-1} in spectra of the ligands are assigned to υ_{asym} and υ_{sym} of terminal NH_2. These bands are present in the spectra of the complexes as well, indicating non-involvement of this group in coordination.

Coordination via the azomethine nitrogen is inferred by the following observations. The absorption due to C=N of the free ligand at 1591 cm^{-1} (TSC^1), 1593 cm^{-1} (TSC^2), and 1595 cm^{-1} (TSC^3) in spectra of the complexes indicates coordination of azomethine nitrogen. Coordination of the thiosemicarbazone ligands to ruthenium ion through azomethine nitrogen is expected to change the electron density in the azomethine and thus alters $\upsilon_{(C=N)}$ to 1596 cm^{-1}, **1**; 1589 cm^{-1}, **2**; and 1596 cm^{-1}, **3** after complexation, indicating coordination of azomethine nitrogen to ruthenium ion.

The $\upsilon_{(N-N)}$ bands of the ligands are at 1053 cm^{-1} (TSC^1), 1062 cm^{-1} (TSC^2), and 1111 cm^{-1} (TSC^3). The change in frequency of these bands 1093 cm^{-1}, **1**; 1093 cm^{-1}, **2**; and 1090 cm^{-1}, **3** in spectra of the complexes provides evidence for coordination via azomethine nitrogen [30]. A strong band at 3151 cm^{-1}, **1**; 3155 cm^{-1}, **2**; and 3181 cm^{-1}, **3** attributed to $\upsilon_{(N-H)}$ of –NH–N=C in spectra of free ligands is not present in spectra of metal complexes [31].

The free ligands display $\upsilon_{(C=S)}$ absorption at 819 cm^{-1} (TSC^1), 831 cm^{-1} (TSC^2) and 838 cm^{-1} (TSC^3). This band is also not present in spectra of the complexes. However, new bands are present at 1541 cm^{-1}, **1**; 1542 cm^{-1}, **2**; 1548 cm^{-1}, **3**; 1020–1036 cm^{-1}, **1** and 727 cm^{-1}, **1**; 750 cm^{-1}, **2**; and 742 cm^{-1}, **3** which are assigned to the new azomethine group –C=N–, –C–O and–C–S, respectively. The disappearance of $\upsilon_{(C=S)}$ and $\upsilon_{(N-H)}$ in **1–3** confirm that TSC ligands coordinate in the thiol form. Bands due to –SH are not present in spectra of **1–3**. These observations indicate the thiolization of –NH–C=S and subsequent deprotonation before coordination. A strong band was obtained at 1254 cm^{-1} in free TSC^1, assigned to phenolic –C–O absorption. On complexation, this band shifted to higher frequency at 1286 cm^{-1}, indicating coordination of TSC^1 through the phenolic oxygen [32]. This is further confirmed by disappearance of the $\upsilon_{(ph-C-OH)}$ broad band $\upsilon_{(OH)}$ at 2967 cm^{-1} in **1**, indicating deprotonation of the phenol prior to coordination through the deprotonated oxygen; $\upsilon_{(OH)}$ of the phenolic group in ligand spectra disappears in the spectrum of **1** and an increase in frequency of phenolic C–O vibration from ligand (1261–1278 cm^{-1}) to metal complex (1313–1319 cm^{-1}) is observed. These results suggest coordinating phenolic oxygen.

In all of the complexes, a strong band at 1944 cm^{-1}, **1**; 1955 cm^{-1}, **2**; and 1935 cm^{-1}, **3** is due to terminally coordinated carbonyl and is observed at higher frequency than in the

precursor complexes [RuHCl(CO)(PPh_3)$_3$] (1928 cm^{-1}). Characteristic absorptions due to triphenylphosphine were also observed for the complexes in their expected regions, 1433–1438 cm^{-1}, 1090–1093 cm^{-1}, 750–794 cm^{-1}, and 518–526 cm^{-1}. Replacement of hydride in the starting complexes by TSC has been confirmed by the absence of a band at 2020 cm^{-1} in all the complexes [33].

Spectra of the complexes show that TSC^1 is coordinated tridentate to ruthenium via azomethine nitrogen (C=N), phenolic oxygen, and sulfur; TSC^2 and TSC^3 coordinate bidentate to ruthenium via azomethine nitrogen (C=N) and sulfur. C=N/SH vibrations have different wavenumbers in the FT-IR spectra of **1–3**, respectively.

Bands are assigned to $\upsilon_{(M-N)}$, further supporting coordination of the azomethine nitrogen. In the complexes the medium intensity band at 518–526 cm^{-1} is attributed to Ru–N [34]. In the low frequency region 439 cm^{-1} is attributed to Ru–O [35].

3.2.2. ^{1}H and ^{31}P NMR spectra. The ligand-to-metal bonding is further supported by ^{1}H and ^{31}P NMR spectra. The TSC ligands and the complexes are very soluble in DMSO and so their NMR spectra were obtained in DMSO-d_6. The ^{1}H NMR spectral results obtained for TSC^n and **1–3** in DMSO-d_6 with their assignments are given in the experimental section.

Signals of phenolic proton appear at 11.38 ppm (TSC^1) and NH protons at 9.16 ppm (TSC^1), 9.51 ppm (TSC^2), and 9.28 ppm (TSC^3) in ^{1}H NMR spectra of the ligands. These signals are not present in spectra of the complexes, indicating deprotonation of these groups. The proton resonance as a singlet at δ = 11.38 ppm in the spectra (TSC^1) due to the –OH proton disappeared in the spectra of **1**. The absence of OH resonance in **1** indicates deprotonation of the phenolic group of the thiosemicarbazone on complexation and coordination to ruthenium through phenolic oxygen. In spectra of **1–3**, a sharp singlet at 8.38 ppm, **1**; 8.37 ppm, **2**; and 8.30 ppm, **3** has been assigned to azomethine proton (–HC=N). The positions of azomethine signal in the complexes are shifted to a lower field compared to free ligands at 8.18 ppm (TSC^1), 8.16 ppm (TSC^2), and 8.04 ppm (TSC^3), indicating coordination through the azomethine nitrogen. In spectra of **1–3**, a multiplet observed at 6.74–8.08 ppm, **1**; 6.79–7.96 ppm, **2**; and 6.74–7.17 ppm, **3** is assigned to aromatic protons and the phenyl group of triphenylphosphine.

Resonances of terminal NH_2 in **1–3** are seen in the same positions as in ligand spectra 3.29–3.34, confirming the non-involvement of this group in coordination. The resonances for the methoxy protons are singlet at 3.8 ppm in TSC^1 and **1** with no significant change.

In the ^{1}H NMR spectra of **1–3** all indications are that the TSC ligands are anionic (evidenced by the absence of the –NH– protons). Enolization of thiocarbonyl group is indicated by the singlet present at 10.4 ppm in spectra of the ligand, attributed to –C–SH protons of thioamide group of TSC. The absence of thionyl group in the complexes indicates deprotonation of this group on coordination through thionyl sulfur. The absence of signals ascribed to –SH is consistent with the idea that in solution, as in the solid state, the ligand exists as the deprotonated thiol tautomer [36].

The ^{31}P NMR spectra showed one peak in **1** and **3** at 27.61 and 36.73 ppm, respectively, indicating that the triphenylphoshine groups are *trans* in these complexes [37]. In **2**, it is observed as peaks at 55.01 and 43.52 ppm, indicating that the triphenylphosphine groups are *cis*.

3.2.3. Electronic spectra. Electronic spectral assignments of **1–3**, given in the experimental section, showed two and three bands at 333–324 nm. The ground state of ruthenium(II)

is $^1A_{1g}$, arising from the t^6_{2g} configuration in an octahedral environment. Excited state corresponding to the $t^5_{2g}e^1_g$ configuration are $^3T_{1g}$, $^3T_{2g}$, $^1T_{1g}$, and $^1T_{2g}$. Hence, four bands corresponding to the transitions $^1A_{1g}\rightarrow{}^3T_{1g}$, $^1A_{1g}\rightarrow{}^3T_{2g}$, $^1A_{1g}\rightarrow{}^1T_{1g}$, and $^1A_{1g}\rightarrow{}^1T_{2g}$ are possible, in order of increasing energy. The electronic spectra of the complexes show several absorptions in the ultraviolet region.

Bands at 281–284 nm in all the complexes may be assigned to Ru $(4d\pi)\rightarrow\pi^*$ (imine) (MLCT) transition. The other bands below 275 nm are due to intraligand transitions occurring within ligand orbitals. These bands are seen in the spectra of the ligands also but at a slightly lower wavelength, indicating the coordination of the ligands to ruthenium. The pattern of the electronic spectra of all the complexes indicates the presence of an octahedral geometry around ruthenium(II) [33].

3.2.4. Fluorescence-based spectra. The photoluminescence properties were studied at room temperature for **1–3** either doped in DMSO or solid matrix of ethyl cellulose. The fluorescence data are given in table 1. All of the complexes in the solution phase were excited in the range 235–341 nm. The emissions were observed as a broad and intense band from 340 to 550 nm, attributed to the spin-allowed ligand-centered $\pi\rightarrow\pi^*$ bands in the UV region of the excitation spectra [38, 39]. Intense emission maxima were observed at 382, 358, 387, and 389 nm for **1**, **2**, **3**, and **4**, respectively. The emission maximum of **2** which had only one phenolic group in its thiosemicarbazone ligand was the lowest at 358 nm. The emission maximum of **4** which had a thiophene was the highest at 389 nm. Mishra *et al.* reported that the attachment of the 2-thienyl group in $[Ru(tpy\text{-}th)_2]^{2+}$ (th = thiophene) causes a red shift in the absorption maximum which consequently will cause a red shift in the emission maximum [38]. This red shift indicates that the thiophene has very strong electronic interactions with Ru-to-ligand charge transfer states and strongly stabilizes these MLCT states. The thiosemicarbazone binds the metal center via the nitrogen and oxygen forming five- and six-membered chelate rings in the case of **1**. The relatively higher emission maximum of **1** when compared with **2** can be attributed to these rings and the hindered rotational movements. Thus, by doping of **1** in solid ethyl cellulose membrane for oxygen sensing, no significant red shift in the excitation and emission maxima was observed. However, in the case of **4**, by the doping of the complex into the solid matrix, the structure became more rigid, preventing rotational movements and causing a red shift of 60 nm from 280 to 340 nm in its excitation maximum (figure 3).

Table 1. Fluorescence-based data in solution of DMSO and in solid matrix of EC.

Complexes	λ_{max} for excitation, nm	λ_{max} for emission, nm	Stokes shift	Fluorescence intensity (100% N_2)	Fluorescence intensity (100% O_2)	Relative signal change, %	Matrix
1	282, 341	382	100	575	280	51	DMSO
2	235, 280	358	74	410	360	13	DMSO
3	305	387	120	350	300	14	DMSO
4	309	389	80	480	420	13	DMSO
1	320, 340(s)	375(s), 387	67	890	710	20	EC
4	330, 345(s)	380(s), 395	65	815	760	7	EC

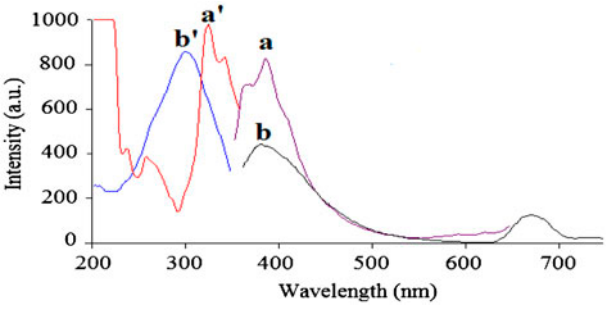

Figure 3. Emission and excitation spectra for **4** and in solid matrix of ethyl cellulose (a and a′) and in solution of DMSO (b and b′).

The Stoke's shift values of the complexes were also calculated (table 1). All of the complexes exhibited relatively high Stoke's shifts ranging from 65 to 120 nm, allowing the emitted fluorescence photons to be easily distinguished from the excitation photons, and is of great importance for future sensor studies.

3.2.5. Oxygen-sensing studies. Triplet oxygen is able to quench fluorescence of ruthenium complexes via collisions with the fluorophore in its excited state leading to a non-radiative energy transfer. This is called "dynamic fluorescence quenching." The degree of quenching relates to the frequency of collisions, and therefore to the concentration, pressure, temperature, and matrix material of the sensor. In our case, the oxygen-sensing properties were examined both for the solution phase (DMSO) and for the ethyl cellulose matrix. In the solution phase, **1** exhibited the highest quenching efficiency for oxygen with a relative signal change of 51% after exposure to 100% N_2 (g) and 100% O_2 (g). However, in the solid ethyl cellulose matrix the relative signal change was only 22% (figure 4). This can be attributed to the diffusion-controlled mechanism of quenching where the microstructure and porosity of the sensing films influence the oxygen permeability. Complex **1** is promising for future oxygen sensor designs and the relative signal change can be enhanced by utilization of different matrices or by modification of the current matrix.

3.3. *Antimicrobiological activities*

Complexes **1–3** were tested for their *in vitro* antibacterial and antifungal activity by disk diffusion method [28, 29] with five Gram-positive bacteria *B. subtilis* ATCC 11774, *S. aureus* ATCC 25923, *S. pyogenes* ATCC 19615, *S. aureus* (clinical isolate), and *S. agalactiae* (clinical isolate), four Gram-negative bacteria *E. coli* ATCC 25922, *E. cloacae* ATCC 23355, *P. aeruginosa* ATCC 27853, and *P. aeruginosa* (clinical isolate), and one fungal strain *C. albicans* ATCC 10231. Ofloxacin, amoxycillin/clavulanic acid (2 : 1), imipenem, erythromycin, and nystatin were used as standard drugs. Table 2 shows the antimicrobial activity of standard antibiotics against the test micro-organisms. The ruthenium complexes did not show any inhibition zone against micro-organisms at the concentration (50, 75, and 100 μg/6 mm paper disk) evaluated in this work. Some Ru(II) thiosemicarbazone complexes do not exhibit antimicrobial activity against medically important bacterial and fungal strains, and therefore research results are obtained by Beckford *et al.* [40, 41] that shows parallels with the results of this study.

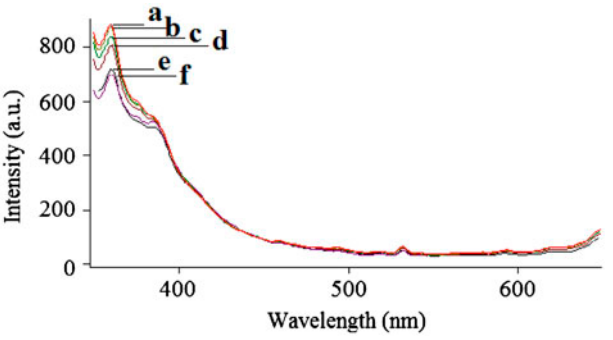

Figure 4. Emission spectra for **4** in solid matrix of ethyl cellulose (a) 0.0%, (b) 10%, (c) 20%, (d) 40%, (e) 60%, (f)100%, and O_2 (g).

Table 2. Antimicrobial activities of standard antibiotics.

	Inhibition zone diameter (mm)[a]				
Tested organisms	E (15)	AMC (30)	OFX (5)	IPM (10)	N (60)
Bacillus subtilis ATCC 11774	>30	28	27	>30	nt
Staphylococcus aureus ATCC 25923	20	30	22	>30	nt
Streptococcus pyogenes ATCC 19615	24	24	16	28	nt
Staphylococcus aureus[b]	18	16	22	>30	nt
Streptococcus agalactiae[b]	28	>30	22	>30	nt
Escherichia coli ATCC 25922	12	18	28	20	nt
Enterobacter cloacae ATCC 23355	*r*	19	28	23	nt
Pseudomonas aeruginosa ATCC 27853	*r*	*r*	13	22	nt
Pseudomonas aeruginosa[b]	*r*	*r*	23	24	nt
Candida albicans ATCC 10231	nt	nt	nt	nt	22

Notes: E: erythromycin; AMC: amoxycillin/clavulanic acid (2 : 1); OFX: ofloxacin; IPM: imipenem; N: nystatin; nt: not tested; and *r*: resistance.
[a]μg/6 mm paper disk.
[b]Clinical isolates.

4. Conclusion

This paper describes the synthesis, structural, and spectral characterization of four TSCs of 2-hydroxy-3-methoxybenzaldehyde, 3-hydroxybenzaldehyde, 3,4-dihydroxybenzaldehyde, thiophene-2-carbaldehyde and their ruthenium complexes and some reactivities of these complexes.

The spectroscopic studies showed one ligand is coordinated to ruthenium as a tridendate ligand coordinating via the azomethine nitrogen (C=N), phenolic oxygen, and sulfur in **1**, whereas second, third, and fourth ligands are coordinated to the central metal as a bidentate ligand, coordinating via azomethine nitrogen (C=N) and sulfur in **2** and **3**. The new ruthenium complexes were not found to have any toxic activity against the Gram-negative and Gram-positive bacteria and also fungus. When compared with other complexes, **1** exhibited higher sensitivity to gaseous oxygen and can be employed as optical chemical sensor for further studies. The relative signal change when exposed to oxygen gas was promising and 51% in solution phase. By the utilization of different matrices or by applying modification procedures, the diffusion of oxygen to the relative signal change in the solid matrix can be enhanced.

Acknowledgements

This study was supported by project number *2011.KB. FEN.047* and *2012.KB. FEN.047* from Dokuz Eylul University Rectorship, Scientific Research Project Coordination Center. We also thank the Graduate School of Natural and Applied Sciences, Dokuz Eylul University, EBILTEM, Ege University for NMR analysis, and TUBITAK, for elemental analysis.

References

[1] G.F. de Sousa, C.A.L. Filgueiras, M.Y. Darensbourg, J.H. Reibenspies. *Inorg. Chem.*, **31**, 3044 (1992).
[2] R. Prabhakaran, R. Karvembu, T. Hashimoto, K. Shimizu, K. Natarajan. *Inorg. Chim. Acta*, **358**, 2093 (2005).
[3] A.R. Cowley, J.R. Dilworth, P.S. Donnelly, J.W. Shore. *Dalton Trans.*, 748 (2003).
[4] C. Paek, S.O. Kang, J. Ko, P.J. Carroll. *Organometallics*, **16**, 4755 (1997).
[5] S. Kannan, M. Sivagamasundari, R. Ramesh, Y. Liu. *J. Organomet. Chem.*, **693**, 2251 (2008).
[6] T.S. Lobana, R. Sharma, G. Bawa, S. Khanna. *Coord. Chem. Rev.*, **253**, 977 (2009).
[7] J.S. Casas, M.S. Garcia-Tasende, J. Sordo. *Coord. Chem. Rev.*, **209**, 197 (2000).
[8] M.J.M. Campbell. *Coord. Chem. Rev.*, **15**, 279 (1975).
[9] F.J. Giles, P.M. Fracasso, H.M. Kantarjian, J.E. Cortes, R.A. Brown, S. Verstovsek, Y. Alvarado, D.A. Thomas, S. Faderl, G. Garcia-Manero, L.P. Wright, T. Samson, A. Cahill, P. Lambert, W. Plunkett, M. Sznol, J.F. DiPersio, V. Gandhi. *Leuk. Res.*, **27**, 1077 (2003).
[10] A. Kolocouris, K. Dimas, C. Pannecouque, M. Witvrouw, G.B. Foscolos, G. Stamatiou, G. Fytas, G. Zoidis, N. Kolocouris, G. Andrei, R. Snoeck, E.D. Clercq. *Bioorg. Med. Chem. Lett.*, **12**, 723 (2002).
[11] G. Aguirre, L. Boiani, H. Cerecetto, M. Fernández, M. González, A. Denicola, L. Otero, D. Gambino, C. Rigol, C. Olea-Azar, M. Faundez. *Bioorg. Med. Chem.*, **12**, 4885 (2004).
[12] S. Sharma, F. Athar, M.R. Maurya, A. Azam. *Eur. J. Med. Chem.*, **40**, 1414 (2005).
[13] D.L. Klayman, J.P. Scovill, J.F. Bartosevich, J. Bruce. *J. Med. Chem.*, **26**, 35 (1983).
[14] N.C. Kasuga, K. Sekino, C. Koumo, N. Shimada, M. Ishikawa. *J. Inorg. Biochem.*, **84**, 55 (2001).
[15] J.G. Da Silva, L.S. Azzolini, S.M.S.V. Wardell, J.L. Wardell, H. Beraldo. *Polyhedron*, **28**, 2301 (2009).
[16] I.C. Mendes, M.A. Soares, R.G. Dos Santos, C. Pinheiro, H. Beraldo. *Eur. J. Med. Chem.*, **44**, 1870 (2009).
[17] K. Alomar, A. Landreau, M. Kempf, M.A. Khan, M. Allain, G. Bouet. *J. Inorg. Biochem.*, **104**, 397 (2010).
[18] S.K. Chatttopadhyay, S. Gosh. *Inorg. Chim. Acta*, **131**, 15 (1987).
[19] P.J. Dyson, G. Sava. *Dalton Trans.*, 1929 (2006).
[20] B. Seven, T. Demirdoven, H. Yildirim, D.O. Demirkol, E. Subasi, E. Sahin, S. Timur. *J. Macromol. Sci., Part A: Pure Appl. Chem.*, **50**, 392 (2013).
[21] H. Yildirim, E. Guler, M. Yavuz, N. Ozturk, P.K. Yaman, E. Subasi, E. Sahin, S. Timur. *Mater. Sci. Eng. C* (accepted August 2014).
[22] O. Oter, K. Ertekin, S. Derinkuyu. *Mater. Chem. Phys.*, **113**, 322 (2009).
[23] M.Z. Ongun, O. Oter, G. Sabanci, K. Ertekin, E. Celik. *Sens. Actuators, B*, **183**, 11 (2013).
[24] O. Oter, K. Ertekin, O. Dayan, B. Cetinkaya. *J. Fluoresc.*, **18**, 269 (2008).
[25] D.D. Perrin, W.L.F. Armarego, D.R. Perrin. *Purification of Laboratory Chemicals*, 2nd Edn, Pergamon, Oxford (1980).
[26] D.L. Klayman, A.J. Lin, N. Acton, J.P. Scovill, J.M. Hoch, W.K. Milhous. *J. Nat. Prod.*, **47**, 715 (1984).
[27] J.P. Scovill. *Phosphorus, Sulfur Silicon Relat. Elem.*, **60**, 15 (1991).
[28] C.L. Clark, M.R. Jacobs, P.C. Appelbaum. *J. Clin. Microbiol.*, **36**, 3579 (1998).
[29] W.R. Kirkpatrick, T.M. Turner, A.W. Fothergill, D.I. McCarthy, S.W. Redding, M.G. Rinaldi, T.F. Patterson. *J. Clin. Microbiol.*, **36**, 3429 (1998).
[30] A. Manimaran, C. Jayabalakrishnan. *J. Adv. Res.*, **3**, 233 (2012).
[31] K. Sampath, S. Sathiyaraj, G. Raja, C. Jayabalakrishnan. *J. Mol. Struct.*, **1046**, 82 (2013).
[32] K. Natarajan, R.K. Poddar, U. Agarwala. *J. Inorg. Nucl. Chem.*, **39**, 431 (1977).
[33] M. Sivagamasundari, R. Ramesh. *Spectrochim. Acta, Part A*, **66**, 427 (2007).
[34] S. Manivannan, R. Prabhakaran, K.P. Balasubramanian, V. Dhanabal, R. Karvembu, V. Chinnusamy. *Appl. Organomet. Chem.*, **21**, 952 (2007).
[35] K. Nakamoto, N. Ohkaku. *Inorg. Chem.*, **10**, 798 (1971).
[36] S. Das, S. Sinha, R. Britto, K. Somasundaram, A.G. Samuelson. *J. Inorg. Biochem.*, **104**, 93 (2010).
[37] C. Rodrigues, A.A. Batista, R.Q. Aucélio, L.R. Teixeira, L.D.C. Visentin, H. Beraldo. *Polyhedron*, **27**, 3061 (2008).
[38] A. Mishra, E. Mena-Osteritz, P. Bäuerle. *Beilstein J. Org. Chem.*, **9**, 866 (2013).

[39] J.G. Małecki, A. Maron, M. Serda, J. Polanski. *Polyhedron*, **56**, 44 (2013).
[40] F.A. Beckford, J. Thessing, M. Shaloski Jr, P.C. Mbarushimana, A. Brock, J. Didion, J. Woods, A. Gonzalez-Sarrías, N.P. Seeram. *J. Mol. Struct.*, **992**, 39 (2011).
[41] F.A. Beckford, A. Stott, A. Gonzalez-Sarrías, N.P. Seeram. *Appl. Organomet. Chem.*, **27**, 425 (2013).